arXiv:1607.00449v2 [physics.atom-ph] 7 Jul 2016

Theoretical Simulation of ^{87}Rb Absorption Spectrum in a Thermal Cell

Cheng Hong,[1,2] Zhang Shan-Shan,[1,2] Xin Pei-Pei,[1,2] Cheng Yuan,[1,2] and Liu Hong-Ping[1,2]

[1]*State Key Laboratory of Magnetic Resonance and Atomic and Molecular Physics, Wuhan Institute of Physics and Mathematics, Chinese Academy of Sciences, Wuhan 430071, People's Republic of China*

[2]*University of Chinese Academy of Sciences, Beijing 100049, People's Republic of China*

(Dated: July 8, 2016)

In this paper, we present a theoretical simulation of ^{87}Rb absorption spectrum in a thermal cm-cell which is adaptive to the experimental observation. In experiment, the coupling and probe beams are configured to copropagate but perpendicular polarized, making up to five velocity selective optical pumping (VSOP) absorption dips able to be identified. A Λ-type electromagnetically induced transparency (EIT) is also observed for each group of velocity-selected atoms. The spectrum by only sweeping the probe beam can be decomposed into a combination of Doppler-broadened background and three VSOP dips for each group of velocity-selected atoms, companied by an EIT peak. This proposed theoretical model can be used to simulate the spectrum adaptive to the experimental observation by non-linear least-square fit method. The fit for high quality of experimental observation can determine valuable transition parameters such as decaying rates and coupling beam power accurately.

PACS numbers: 42.50.Gy, 32.70.Jz, 32.10.Fn, 32.80.Xx

I. INTRODUCTION

Laser-atom interaction can control the quantum interference properties between atomic states, which has various significant applications in many fields. For example, recently, coherence and interference effects in atomic systems such as coherent population trapping (CPT) [1, 2], refractive index enhancement [3], electromagnetically induced transparency (EIT) [4–12], electromagnetically induced absorption (EIA) [13–19] and velocity selective optical pumping (VSOP) [20–22] have been widely applied in atomic clock [23], squeezing of light [24], light storage [25, 26] and quantum computation [27]. Particularly, the theoretical and experimental investigations on EIT in atomic systems are of enhanced interest in scientific researches. EIT was also studied in the atomic ensemble[12], atom-molecule systems [11], and solid-state systems [28–31].

Unlike EIT in simple three-level Λ, V and cascade (ladder)-type atomic systems [16, 32–35], however, most alkali atoms have a complicated energy level structure instead of following an ideal model and the Doppler broadening causes many states involved in the transitions, for example, four [36, 37], five [38, 39], even six level [40, 41] systems having been studied. The D_2 transition of Rb consisting of two ground hyperfine levels and four excited levels forms a six-level scheme system. The separations of the upper hyperfine levels are less than the Doppler broadening of the transition in the room temperature, causing more extra satellite dips also observed due to Doppler shifted along with the EIT peak in the probe transmission profile [21, 22, 42].

These velocity selective resonances result in complexity of the final spectrum and difficulty in their analysis. For example, Maguire *et al.* numerically calculated the optical Bloch equations by taking into the optical effects and the simulated spectra could reproduce the main features of the observed saturation absorption spectra of ^{85}Rb D_2 transition [43]. Bhattacharyya *et al.* studied velocity selective resonance dips along with EIT peak observed in the experiment by solving the density matrix equations of a Λ-type five-level system [6, 44–47]. Applying the perturbation method to the optical Bloch equations, valuable information for induction of EIA was obtained for a closed multilevel $F_g = 1 \rightarrow F_e = 2$ transition in the Hanle configuration [42]. Similarly, by solving the rate equations, Krmpot *et al.* could well identify spectral position and intensity for atoms with different velocities [48]. Ray *et al.* carried out a detailed theoretical analysis of the coherent process by solving the density matrix formulation including all orders of pump and probe powers without any assumptions [49].

However, all of the theories and simulations have to depend on a series of accurate given dynamical parameters such as decay rates and temperature, etc.. Due to the complexity of the atomic multi-levels and uncertainty in laser parameters, most of time, it is difficult to present a simulation comparable with the experiment with high quality. In this paper, rather than starting from the theory based on the Bloch equations, we propose a semiempirical model to numerically explain the experimental observation of the multi-level system of ^{87}Rb D_2 line. The model with varied dynamical parameters can be adaptive to the experimental observation and can give exact coincidence with the observed spectral profile and details. The EIT peak signal stemming from the background of one VSOP absorption dip is also well resolved. The theoretical model is constructed from the main concerned physical processes in the Λ-type EIT with both coupling and probe beams copropagating but perpendicularly polarized, namely, the spectral analysis should consider the Doppler-broadening and Doppler-free processes at the same time.

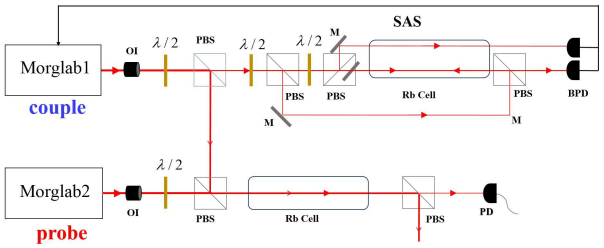

FIG. 1: (Color online) Experimental setup for EIT spectral measurement. PBS: polarizing beam splitter; OI: optical isolator; M: mirror; $\lambda/2$: half wave plate; $\lambda/4$: quarter wave plate; PD: photo detector; SAS: saturation absorption spectroscopy setup.

II. EXPERIMENT

Many works have been done for the observation of the Λ-type EIT for ^{87}Rb [50–52], but to obtain high quality of spectral data for the theoretical analysis, we have to re-investigate the experimental observation. The experimental setup is shown in Fig. 1. Two filter-tuned, cateye refletor feedback external cavity diode lasers (Moglabs) with line-widths < 1 MHz are used in the experiment. One is used to couple hyperfine levels of the ground $^5S_{1/2}$ and excited $^5P_{3/2}$ states of the ^{87}Rb isotope (D_2 line in Rb), and the other one serves as a prober to monitor the transparency of the laser through the Rb vapor. The pump laser beam is split into two parts where the part transmitted through a polarizing beam splitter (PBS) is sent to a Doppler-free saturation absorption set-up (SAS) for locking the laser frequency. At the same time, the pump laser is also partly reflected by the PBS and sent through the sample cell for the EIT experiment as coupling beam. The pumping laser can be locked to any possible hyperfine and crossover transition peak with a long term frequency stability less than 1 MHz.

In a similar way, the probe laser beam transmitted through the PBS serves as the probe beam in the EIT experiment. The coupling and probe laser beams copropagate through the Rb cell, and their polarizations are linear and mutually perpendicular. The coupling and probe laser beams are adjusted to overlap almost completely throughout the total length of the cell. The coupling beam size is around 2.5 mm^2. After the Rb cell, the probe beam was extracted by another PBS and detected by a photodiode. The transmission of the probe laser was detected with its frequency swept across the $^2P_{3/2}$ levels from the ground state $F = 1$. The laser intensities can be controllable by combination of half-wave plate and PBS.

The cylindrical shaped Rb vapor cell is made of pyrex glass and has a size of length 7.5 cm and diameter 2.5 cm. The pressure inside is 10^{-6} Torr at room temperature ($\sim 25°$C) without any buffer gas. The cell filled with both isotopes of Rb in their natural abundances ^{85}Rb (72%) and ^{87}Rb (28%). We have not applied any magnetic field shielding outside the Rb vapor cell since the energy level shifting induced by the earth's magnetic field (~ 0.5 Gauss) is less than 0.5 MHz.

III. THEORY

We considered a Λ-type five-level atomic system interacting with two lasers as shown in Fig. 2. The levels $|1\rangle, |2\rangle$ are the two hyperfine levels in the ground state $^5S_{1/2}$ and the levels $|3\rangle, |4\rangle, |5\rangle$ are the three closely spaced hyperfine levels in the excited state $^5P_{3/2}$. The strong coupling laser is frequency locked to one of the ground level $|2\rangle$ to $\rightarrow |j\rangle$ ($j = 4, 5$) or their crossover transition. While the weak probe beam scans over all the excited levels $|3\rangle, |4\rangle, |5\rangle$ from the other ground level $|1\rangle$, corresponding to transitions from $F = 1$ to $F' = 0, 1, 2$ states. The transitions $|1\rangle \rightarrow |j\rangle$ ($j = 3, 4, 5$) and $|2\rangle \rightarrow |j\rangle$ ($j = 4, 5$) are dipole-allowed while the transitions between the other levels are dipole-forbidden [24].

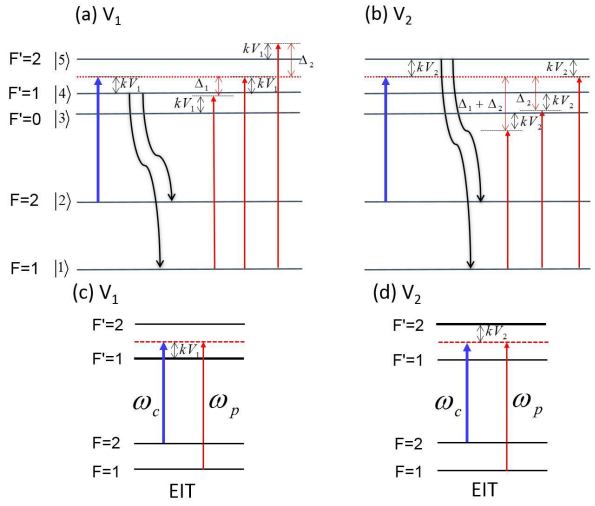

FIG. 2: (Color online) The energy diagram and spectral assignment of the observed spectrum. (a) and (b) are the level schemes for the V_1 and V_2 velocity groups, respectively. The blue solid line indicates the couple beam frequency ω_c locked at the $F = 2$ to $F' = \text{CO}_{1-2}$ while the weak (red colored) line indicates the probe beam scanning from the ground level $F = 1$ to the excited level $F' = 0, 1, 2$. (c) and (d) are the level schemes to show the formation of the EIT for V_1 and V_2 velocity groups.

Due to Doppler broadening, the frequency-fixed coupling laser can populate two distinct velocity groups of atoms to the upper hyperfine levels $F' = 1, 2$ from the ground level $F = 2$, denoted as V_1 and V_2, respectively. These populations on excited states will decay to the two ground hyperfine levels $F = 1, 2$ by spontaneous emission. We are interested in the velocity selective population on the $F = 1$ ground level. The copropagated weak probe laser has an additional response for these veloc-

ity selective atoms. This additional response is superimposed on a Doppler background. Finally, VSOP dips can be observed in the probe transmission profile at Doppler shifted frequencies, as well as EIT signals.

Considering the VSOP signal is much narrower than the Gaussian-broadening, we can omit the convoluting process as an approximation. So here we only consider the convolution of EIT with Gaussian-broadening. Therefore, we can approximate the final spectrum as the sums of absorption VSOPs and transparency EIT superimposed on the Doppler broadening. The Doppler background is mathematically expressed by Gaussian distribution function

$$G(\omega_p) \propto e^{-\frac{v^2}{u^2}} \tag{1}$$

with the most probable velocity defined to be $u = (2k_BT/m_{Rb})^{1/2}$ and v satisfying the relation $\omega_p = \omega_{1j}(1-\frac{v}{c})$.

The EIT signal has the form [53]

$$EIT(\Delta_p) \propto \mathrm{Im}\int \frac{1}{\frac{(\Omega_c/2)^2}{(\Delta_p+\Delta_c)+\frac{\omega_p-\omega_c}{c}v+i\gamma_c} - (\Delta_p+\frac{\omega_p}{c}v+i\gamma_p)} \times e^{-\frac{v^2}{u^2}}dv \tag{2}$$

with Doppler broadening considered. If the Doppler-broadening can be ignored, we can easily set the Gaussian-broadening to zero and the formula is reduced to a standard Doppler-free EIT. Here Ω_c is the Rabi frequency for the coupling laser, Δ_p and Δ_c the detunings of the probe and coupling laser fields, respectively. Taking the Doppler velocity selective effect into account, $\Delta_c = 0$ for the selected atoms and the EIT occurs at $\omega_p = \omega_c + \Delta$, where $\Delta = 6.835$ GHz is the hyperfine level splitting of the ground state. The numerical skills are used for the integral in Eq. 2 [53].

There are three VSOP dips corresponding to the transition $|1\rangle \rightarrow |j\rangle$ $(j = 3, 4, 5)$ for each velocity group of atoms, and the VSOP has the form of Lorentzian line-type [45, 51]

$$L(\omega_p) \propto \frac{1}{(\omega_p-\omega_{1j})^2+\Gamma_p^2}, \tag{3}$$

where ω_{1j} $(j = 3, 4, 5)$ represents the energy gap corresponding to the transition $|1\rangle \rightarrow |j\rangle$ $(j = 3, 4, 5)$.

The observed spectrum for every group of velocity can be viewed as the superpositions of these three basic line types listed in Eqs. 1-3

$$Spectrum = a_1 \times EIT(\Delta_p) \oplus \sum_{j=3}^{5} a_{2j} \times L(\omega_p) \oplus \sum_{j=3}^{5} a_{3j} \times G(\omega_p), \tag{4}$$

where a_1, a_{2j} and a_{3j} are the combination coefficients.

This formula has a simpler form and it can be easily used to make an analysis for the observed experimental data, especially to perform a least-square fit for extracting some spectral character parameters.

IV. RESULTS AND DISCUSSION

Figure 3 presents the probe transmission spectrum as a function of the probe detuning and the corresponding derivative signal for ^{87}Rb D_2 transition. The power of the pump and probe lasers are around 5 and 0.005 mW, respectively. For the ^{87}Rb-D_2 line, the separation of the two hyperfine levels $(F = 1, 2)$ in the ground state is 6.835 GHz, while the separations between the hyperfine levels $(F' = 0, 1, 2, 3)$ of the excited level are $\Delta_1 = 72.3$ MHz (for $F' = 0$ and 1), $\Delta_2 = 157.2$ MHz (for $F' = 1$ and 2) and $\Delta_3 = 267.1$ MHz (for $F' = 2$ and 3), respectively [54]. We observed five VSOP dips (P_1,P_2,...P_5) and a narrow EIT peak (P_4) superimposed on a Doppler background. The separations of the three velocity-selective absorption dips (P_1, P_2, P_3) on the left side of the EIT peak (P_4) are $-(\Delta_1+\Delta_2)$, $-\Delta_2$, and $-\Delta_1$ with respect to the reference frequency $\omega_p - \omega_c - \Delta = 0$. Another dip ($P_5$) on the right-hand side is at a distance of Δ_2 from the EIT peak.

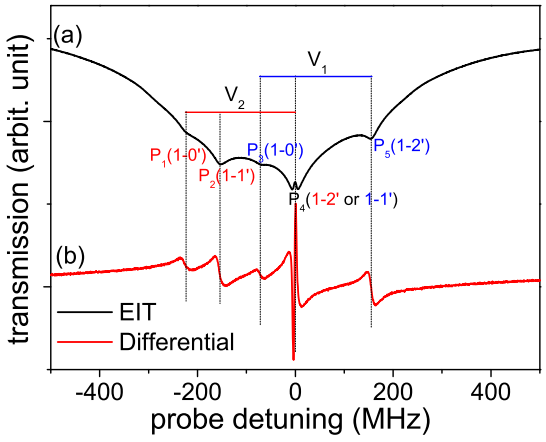

FIG. 3: (Color online) Experimental trace of the five VSOPs and the corresponding differential signal in the Λ-type ^{87}Rb system with the coupling beam locked to $F' = CO_{12}$ at room temperature, while the weak probe laser scans over all the transitions $(F = 1 \rightarrow F' = 0, 1, 2)$.

We can have an analysis for the observed spectrum, namely, the spectrum can be decomposed into the overlapping of two groups of different velocity selection. It is shown in Fig. 4. For each velocity group, the transmission spectrum of the probe laser is modeled as a sum of absorptions of three VSOPs, relatively weighted by a Maxwell-Boltzmann distribution, and one EIT over the

Doppler-broadening, as described in the theory part. In our process, all the weights are replaced by the combination coefficients and assigned to some trial values by visional comparison of the simulation and the experimental trace. They are varied in the least-square fit and arrive at convergent values by iteration algorithm. By switching on and off the corresponding coefficients, we can plot the respective spectral simulations corresponding to the two different velocity groups of atoms (V_1 and V_2), which are shown in Fig. 4(a) and (b). They are summarized again to produce the final simulated absorption spectrum as shown in Fig. 4(c), which coincides with the experimental observation with high quality. From the convergent fitting, we can determine the parameters of γ_c, γ_p for the EIT. The determined values are $\gamma_c = 3$ MHz and $\gamma_p = 6$ MHz, in good agreement with $\gamma_c = (\gamma_{j2} + \gamma_{21})/2 = 3$ MHz, $\gamma_p = (\gamma_{j2} + \gamma_{j1})/2 = 6$ MHz [55], in which γ_{j1} and γ_{j2} equal to the natural decay rate Γ (6 MHz), γ_{21} is the nonradiative decay rate between the ground levels (100 kHz) which is negligible. The parameter Ω_c can also be determined from the EIT peak. It has a value $\Omega_c = 14$ MHz, close to $\Omega_c = 12.7$ MHz estimated from laser power 5 mW and beam diameter $d = 0.2$ cm. In the estimation, the formula $\Omega_c = \mu E/\hbar$ is used, but the beam has an irregular shape and it is difficult to estimate the effective diameter. It should be noted that we can also have fitted Γ_p values for VSOP peaks in every velocity group. Their values are 17, 22 and 25 MHz, respectively. In the fit, the parameters of line center ω_{1j} in Eq. 1 are fixed and all others are varied.

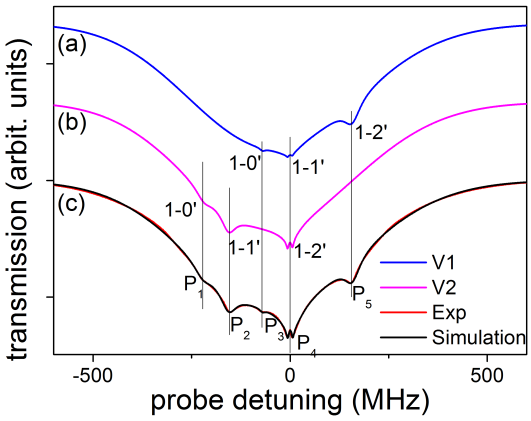

FIG. 4: (Color online) Spectral simulation for the experimental observation. The spectrum can be decomposed into two velocity selective groups V_1 (a), and V_2 (b). The simulation of the total probe absorption spectra is in good agreement with the observation (c).

We also investigate the absorption spectra with the coupling laser locked to different SAS peaks. It is shown in Fig. 5. The detunings of coupling laser are relative to the transition frequency from $F = 2$ to $F' = 2$. We can see that the VSOP dips and the EIA peak also shift over the Doppler background with the coupling frequency shifting, and the frequency translations are the same. It is clearly seen that as the coupling laser being red-detuned ($\delta = -157.2$ MHz) for $F = 2 \rightarrow F' = 2$ transition, the magnitudes of the VSOP peaks belonging to the V_1 velocity selective group of atoms increase, while the other VSOP dips belonging to the V_2 velocity selective group decrease due to the Doppler-broadening weight variation. All absorption spectra are simulated at fitted parameters, in good agreement with the experimental spectrum, and give the same parameter values for γ_c and γ_p, and the determined Ω_c is 17 MHz, very close to the estimated value 17.9 MHz from the coupling laser power 10 mW with beam size $d = 0.2$ cm. The exact coincidence with the experimental observation indicates the reasonableness of the theoretical model as well.

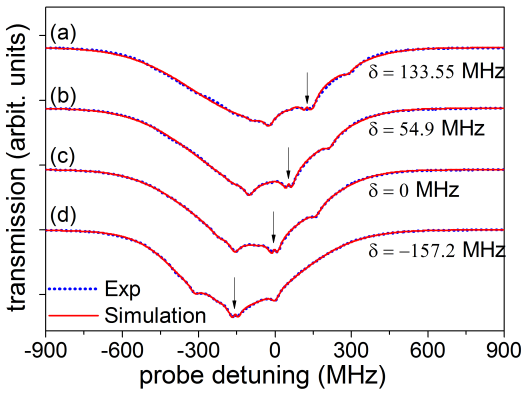

FIG. 5: (Color online) Experimental observation and simulation of the absorption spectra by scanning the probe beam but the coupling beam locked to different excited levels. The shift of the locking frequencies are given relative to the transition $F = 2$ to $F' = 2$ ($\delta = 0$). The coupling laser beam power is fixed at 10 mW.

Finally, we studied the effect of the coupling laser pump power on the VSOP dips and EIT peak for ^{87}Rb atoms. The power varies from 2 mW to 17 mW, which are shown in Fig. 6. In the experiment, the coupling laser frequency is locked to the crossover transition $F = 2$ to CO_{12}. As we know, the power of coupling laser only affects the EIT spectral structure, further separating the EIT peaks, even entering into the region of Autler-Townes splitting. The least-square fit for the spectral data also gives the same parameter values for γ_c and γ_p, but different $\Omega_c = 9$, 11.6 and 23 MHz at power 2, 3 and 17 mW, respectively, which are approaching to the estimated values 8, 9.8 and 23 MHz from the measured power and coupling laser beam waist size $d = 0.2$ cm.

V. CONCLUSION

In this paper, we reinvestigate the EIT and VSOP spectra in a five-level Λ-scheme atomic system of ^{87}Rb atom, where two ground hyperfine states ($F = 1, 2$)

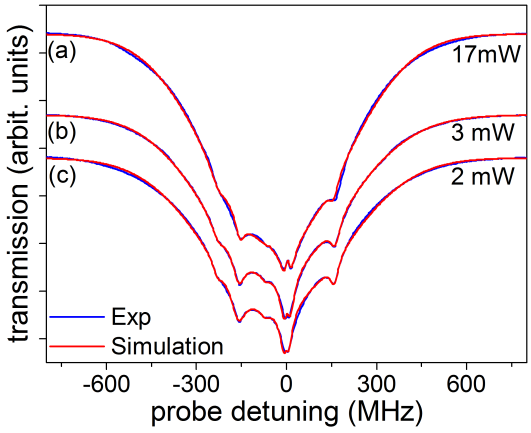

FIG. 6: (Color online) Effect of the coupling laser power on the absorption spectra. The coupling beam is locked to the crossover transition $F = 2$ to CO_{12}. The probe beam power is about 0.005 mW.

of the $^5S_{1/2}$ level and three excited hyperfine states ($F' = 0, 1, 2$) corresponding to $^5P_{3/2}$ level are involved. Rather than starting from the theory based on the Bloch equations, we propose a semiempirical model to numerically explain the experimental observation. It can give exact coincidence for the spectral profile and details.

In our model, we consider EIT and VSOPs separately where the VSOP is supposed to have a Lorentzian-type spectral feature while EIT adopts the standard EIT spectral structure. The effective spectrum can be obtained by the sum of these spectra superimposed on the Doppler-broadening background. The effect of the coupling frequency detuning and coupling beam power on the absorption spectra is also studied. The simulated spectra show fairly good agreement with the experimental findings. It proves the validity of our semiemperical model, and reversely it helps us to extract useful dynamic information from the observed spectrum. This method also can be extended to complicated cases such as the N-, M- or Y-type systems with multi-laser fields [7, 56, 57]. If the VSOP experimental configuration is adopted, principally, we can decompose the physical process as the combination of Doppler-broadening and Doppler-free ones.

Acknowledgments

This work is supported by the MOST 2013CB922003 of the National Key Basic Research Program of China, and by NSFC (No. 91421305, No. 91121005, and No. 11174329).

[1] Aspect A, Arimondo E, Kaiser R, Vansteenkiste N and Cohen-Tannoudji C, 1988. *Phys. Rev. Lett.* **61** 826.
[2] Alzetta G, Moi L and Orriols G, 1979. *Il Nuovo Cimento* **52B** 209.
[3] Fleischhauer M, Keitel C H, Scully M O, Su C, Ulrich B T and Zhu S, 1992. *Phys. Rev. A* **46** 1468.
[4] Kasapi A, Jain M, Yin G Y and Harris S E, 1995. *Phys. Rev. Lett.* **74** 2447.
[5] Harris S E, Field J E and Imamoglu A, 1990. *Phys. Rev. Lett.* **64** 1107.
[6] Hossain M M, Mitra S, Chakrabarti S, Bhattacharyya D, Ray B and Ghosh P N, 2009. *Eur. Phys. J. D* **53** 141.
[7] Joshi A and Xiao M, 2003. *Phys. Lett. A* **317** 370.
[8] Wang J, Kong L B, Tu X H, Jiang K J, Li K, Xiong H W, Zhu Y and Zhan M S, 2004. *Phys. Lett. A* **328** 437.
[9] Sargsyan A, Leroy C, Pashayan-Leroy Y, Mirzoyan R, Papoyan A and Sarkisyan D, 2011. *Appl. Phys. B* **105** 767.
[10] Meng W, Jin-Hai B, Li-Ya P, Xiao-Gang L, Yan-Lei G, Ru-Quan W, Ling-An W, Shi-Ping Y, Zhao-Guang P, Pan-Ming F and Zhan-Chun Z, 2015. *Acta Phys. Sin-ch. Ed.* **64** 154208.
[11] Jing H, Deng Y and Zhang W, 2009. *Phys. Rev. A* **80** 025601.
[12] Jing H, Liu X J, Ge M L and Zhan M S, 2005. *Phys. Rev. A* **71** 062336.
[13] A Lezama S B and Akulshin A M, 1999. *Phys. Rev. A* **59** 4732.
[14] Akulshin A M, Barreiro S and Lezama A, 1998. *Phys. Rev. A* **57** 2996.
[15] Dimitrijević J, Arsenović D and Jelenković B M, 2007. *Phys. Rev. A* **76** 013836.
[16] Fulton D J, Shepherd S, Moseley R R, Sinclair B D and Dunn M H, 1995. *Phys. Rev. A* **52** 2302.
[17] Goren C, Wilson-Gordon A D, Rosenbluh A and Friedmann H, 2004. *Phys. Rev. A* **70** 043814.
[18] Grewal R S and Pattabiraman M, 2015. *J. Phys. B* **48** 085501.
[19] Kim S K, Moon H S, Kim K and Kim J B, 2003. *Phys. Rev. A* **68** 063813.
[20] Wong V, Boyd R W, Stroud C R, Bennink R S and Marino A M, 2003. *Phys. Rev. A* **68** 012502.
[21] Chakrabarti S, Pradhan A, Ray B and Ghosh P N, 2005. *J. Phys. B* **38** 4321.
[22] Moon G and Noh H R, 2008. *Phys. Rev. A* **78** 032506.
[23] Kitching J, Knappe S and Hollberg L, 2002. *Appl. Phys. Lett.* **81** 553.
[24] Zibrov A S, Lukin M D, Nikonov D E, Hollberg L, Scully M O, Velichansky V L and Robinson H G, 1995. *Phys. Rev. Lett.* **75** 1499.
[25] Liu C, Dutton Z, Behroozi C H and Hau L V, 2001. *Nature* **409** 490.
[26] Peng A, Johnsson M, Bowen W P, Lam P K, Bachor H A and Hope J J, 2005. *Phys. Rev. A* **71** 033809.
[27] Scully M O, 1991. *Phys. Rev. Lett.* **67** 1855.
[28] Jing H, Ozdemir S K, Geng Z, Zhang J, Lu X Y, Peng B, Yang L and Nori F, 2015. *Sci. Rep.* **5** 9663.
[29] She Y C, Zheng X J and Wang D L, 2014. *Chin. Phys. B* **23** 124202.
[30] Totsuka K, Kobayashi N and Tomita M, 2007. *Phys. Rev. Lett.* **98** 213904.
[31] Yan X B, Gu K H, Fu C B, Cui C L and Wu J H, 2014.

Chin. Phys. B **23** 114201.
[32] Zeng Z Q, Hou B P, Liu F T and Gao Z H, 2014. *Opt. Commun.* **315** 12.
[33] Jones D E, Franson J D and Pittman T B, 2015. *Phys. Rev. A* **92** 043806.
[34] Wang M, Lu X G, Bai J H, Pei L Y, Miao X X, Gao Y L, Wu L A, Fu P M, Yang S P, Pang Z G, Wang R Q and Zuo Z C, 2015. *Chin. Phys. B* **24** 114205.
[35] Xue Y L, Zhu S D, Liu J, Xiao T H, Feng B H and Li Z Y, 2016. *Chin. Phys. B* **25** 044203.
[36] Taichenachev A V, Tumaikin A M, Yudin and I V, 1999. *Phys. Rev. A* **61** 011802(R).
[37] de Echaniz S R, Greentree A D, Durrant A V, Segal D M, Marangos J P and Vaccaro J A, 2001. *Phys. Rev. A* **64** 013812.
[38] Ottaviani C, Rebić S, Vitali D and Tombesi P, 2006. *Phys. Rev. A* **73** 010301(R).
[39] Wu Y, Saldana J and Zhu Y, 2003. *Phys. Rev. A* **67** 013811.
[40] Agarwal G S and Harshawardhan W, 1996. *Phys. Rev. Lett.* **77** 1039.
[41] Bharti V and Wasan A, 2013. *J. Phys. B* **46** 125501.
[42] Dimitrijević J, Arsenović D and Jelenković B M, 2011. *New J. Phys.* **13** 033010.
[43] Maguire L P, van Bijnen R M W, Mese E and Scholten R E, 2006. *J. Phys. B* **39** 2709.
[44] Bhattacharyya D, Ray B and Ghosh P N, 2007. *J. Phys. B* **40** 4061.
[45] Bhattacharyya D, Bandyopadhyay A, Chakrabarti S, Ray B and Ghosh P N, 2007. *Chem. Phys. Lett.* **440** 24.
[46] Bhattacharyya D, Ghosh A, Bandyopadhyay A, Saha S and De S, 2015. *J. Phys. B* **48** 175503.
[47] Bhattacharyya D, Dutta B K, Ray B and Ghosh P N, 2004. *Chem. Phys. Lett.* **389** 113.
[48] Krmpot A J, Rabasovic M D and Jelenkovic B M, 2010. *J. Phys. B* **43** 135402.
[49] Dey S, Mitra S, Ghosh P N and Ray B, 2015. *Optik* **126** 2711.
[50] Chakrabarti S, Pradhan A, Ray B and Ghosh P N, 2005. *J. Phys. B* **38** 4321.
[51] Mitra S, Hossain M M, Ray B, Ghosh P N, Cartaleva S and Slavov D, 2010. *Opt. Commun.* **283** 1500.
[52] Harris S E, 1997. *Phys. Today* **50** 36.
[53] Chakrabarti S, Ray B and Ghosh P N, 2007. *Eur. Phys. J. D* **42** 359.
[54] Arimondo E, Inguscio M and Violino P, 1977. *Rev. Mod. Phys.* **49** 31.
[55] Wei X G, Wu J H, Sun G X, Shao Z, Kang Z H, Jiang Y and Gao J Y, 2005. *Phys. Rev. A* **72** 023806.
[56] Chen Y, Wei X G and Ham B S, 2009. *J. Phys. B* **42** 065506.
[57] Yang H, Yan D, Zhang M, Fang B, Zhang Y and Wu J H, 2012. *Chin. Phys. B* **21** 114207.